



# Effects on Heat Transfer and Radial Temperature Profile of Non-Isoviscous Vibrational Flow with Varying Reynolds Number

S. K. Mishra<sup>1†</sup>, H. Chandra<sup>2</sup> and A. Arora<sup>1</sup>

<sup>1</sup> Bhilai Institute of Technology, Durg, Chhattisgarh, 491001, India

<sup>2</sup> VEC Lakhanpur, Ambikapur, Chhattisgarh, 497001, India

†Corresponding Author Email: [santosh.mishra@bitdurg.ac.in](mailto:santosh.mishra@bitdurg.ac.in)

(Received March 5, 2018; accepted July 25, 2018)

## ABSTRACT

A valid CFD model is employed to show the impact on heat transfer of one-dimensional laminar non-isoviscous flow through pipe subjected to forced transverse vibration. Through transverse vibration, which produces the chaotic fluid motion and swirling effects, adequate radial mixing across the tube can be achieved which leads to the great addition in heat transfer. Thermal boundary layer developed more quickly and thus, temperature profile developed wilder than steady flow under the effect of vibration in both radial and axial direction, considerably for low Reynolds Number; as Reynolds number increases that effectively reduced. In this study, these impacts are quantitatively exhibited for Newtonian and shear-thinning liquid at various Reynolds numbers; and found that application of superimposed vibrational flow limited to considerably for small: Reynolds number and flow behavior index of shear thinning fluids.

**Keywords:** CFD; Heat transfer coefficient; Vibrational flow; Non-Newtonian flow; Laminar flow.

## NOMENCLATURE

a	wall surface area	t	Time
A	vibration amplitude	T	local temperature
$C_p$	specific heat capacity	$T_{in}$	area-averaged temperature at inlet of pipe
D	pipe diameter	$T_{out}$	area-averaged temperature at outlet of pipe
$E_a$	activation energy	$T_w$	wall temperature
$E_R$	enhancement ratio	$\Delta T_m$	log-mean temperature difference
f	vibration frequency	$T_{VF}$	mean temperature of vibrational flow
Gr	Graetz number	$T_{SF}$	mean temperature of steady flow
h	heat transfer coefficient	w	axial velocity
$h_v$	vibrational heat transfer coefficient	$\bar{w}$	mean axial velocity
k	fluid consistency index	$\dot{x}$	wall velocity in the x direction
$k_o$	pre-exponential factor	x	x-coordinate
L	pipe length	y	y-coordinate
n	flow behaviour index	z	z-coordinate
p	fluid pressure		
$\Delta p$	pressure drop	$\dot{\gamma}$	shear rate
Q	steady-state volumetric flow rate	$\mu$	viscosity
r	radial coordinate	$\mu_{eff}$	effective viscosity
R	pipe radius	$\rho$	fluid density
$R_G$	ideal gas constant	$\theta$	dimensionless temperature
Re	Reynolds number	$\lambda$	thermal conductivity
$Re_v$	vibration Reynolds number		

## 1. INTRODUCTION

Uneven distribution of heat across the tube

subjected to heat transfer produces the wide variation of product sterility and nutritional quality and thence results in undesirable product eminence

(Jung & Fryer, 1999). The challenge is, therefore, Sterilization of fluid nearer to the wall that are having lowest velocities, while not over-processing whereas within the core region of the pipe with most rate, ideally, gets equal heat treatment so healthy the merchandise quality. Therefore, methods are needed, that assures the uniform heat distribution across the tube to promote efficient radial mixing. Better radial mixing of fluid can be achieved through geometry modification of the wall like the incorporation of internal screw-thread structures (Shrirao *et al.*, 2013) or by use of different types of the static mixture (Hobbs & Muzzio, 1997; Saatdjian, Rodrigo, & Mota, 2012). This type of devices has the problem of cleaning that promotes fouling and leads to unhygienic product and modification of pipe wall geometry may involve manufacturing complexities.

Effects of forced vibration, applied in transverse direction on the fluid flowing through a pipe subjected to heat transfer was numerically studied by many researchers and come up with the following conclusion: 1) vibration, satisfactorily increases the radial mixing of fluid depending on the frequency and amplitude because of the swirling effect that leads to more uniform temperature distribution across the tube; 2) Wall heat transfer coefficient can be increased in several fold by varying the vibration parameters and it's also depended on the rheological characteristics of the fluids (Easa & Barigou, 2008; Easa & Barigou, 2010; Tian, 2015).

Thermal boundary layer grow more rapidly under the effects of vibration which considerably reduced the requirement of long length pipe to capture the same effects in the axial direction and for the same heat transfer as in the vibrational flow (Easa & Barigou, 2011).

Easa & Barigou, (2011) has also reported that transverse vibration generates strong spiraling fluid motion that creates cleaning action, as results reduction in fouling of the pipe.

Tian and Barigou (2015) has done the heat transfer analysis in all modes of vibration and concluded that transverse vibration produces more swirling effects responsible for radial mixing of temperature than any other mode of vibrations.

Tian and Barigou (2015) presented that excellent improvement of radial mixing across the tube can be achieved by combining the transverse vibration and a step rotation of oscillation orientations. They have proven that the results obtained from this methods are better than results obtained by the application of well-known Kenics helical static mixer which has the disadvantage of unhygienic fluid processing.

In the current study, a CFD model is employed to research the effects on radial temperature distribution and heat transfer with different Reynolds number of Newtonian and power-law fluid, non-isoviscous, laminar transverse vibrational flow, receiving heat from the wall, maintained at constant temperature.

## 2. METHODOLOGY

### 2.1 Pressure Drop, Velocity Profiles, Fluid Rheology and Fluid Viscosity

Newtonian and inelastic, time-independent non-Newtonian pseudoplastic of the power-law type fluids are considered for the study. The apparent viscosity of the Newtonian fluid is constant at given temperature and pressure but for non-Newtonian fluid, it depends on the wall diameter, shear rate etc. also, the following constitutive equation defines the apparent viscosity of power-law fluids

$$\tau = k\dot{\gamma}^n \quad (1)$$

The apparent viscosity which is the function shear rate,  $\eta$  is then given by

$$\eta = k\dot{\gamma}^{n-1} \quad (2)$$

The velocity profile of fully developed laminar flow through pipe of radius R, of a power-law type fluid is given by expression (3) and this expression is also applicable to Newtonian fluid at  $n = 1$  (Chhabra & Richardson, 1999).

$$w(r) = \bar{w} \left( \frac{3n+1}{n+1} \right) \left[ 1 - \left( \frac{r}{R} \right)^{\frac{n+1}{n}} \right] \quad (3)$$

at  $n = 1$  equation (3) changed in the given form for Newtonian fluid.

$$w(r) = 2\bar{w} \left[ 1 - \left( \frac{r}{R} \right)^2 \right] \quad (4)$$

where  $r$  is radial coordinate and  $\bar{w}$  is the mean axial velocity of flow.

Pressure drop and velocity (Flow rate of constant density fluid flowing from the constant cross-sectional area) can be correlated from the following expression (Steffe, 1996).

$$\text{Newtonian fluid: } Q = \pi R^2 \bar{w} = \frac{\pi \Delta p R^2}{8\mu L} \quad (5)$$

Power-law type fluid:

$$Q = \pi R^2 \bar{w} = \pi \left( \frac{\Delta p}{2kL} \right)^{1/n} \left( \frac{n}{3n+1} \right) R^{\left( \frac{3n+1}{n} \right)} \quad (6)$$

Viscosity of fluid under the non-isothermal condition is greatly influenced by temperature (Kreith & Bohn, 1986), so the variation of viscosity  $\mu$  of Newtonian fluid w.r.t. the temperature was taken into account and given by (Steffe, 1996) Arrhenius model:

$$\mu = k_o \exp \left( \frac{E_a}{R_G T} \right) \quad (7)$$

Further for non-Newtonian fluid, Christiansen & Craig (1962) combined the Arrhenius model (Equation (7)) with the power-law rheological model (Equation (1)) and given the subsequent equation, that is wide accustomed describe the fluid consistency index under the influence of temperature,  $k$ :

$$k = k_o \exp \left( \frac{E_a}{R_G T} \right)^n \quad (8)$$

## 2.2 Temperature Profile

The expression of temperature distribution over the pipe when fluid subjected to continuous heat interaction from pipe wall is given by:

$$w(r) \frac{\partial \theta}{\partial z} = \frac{\lambda}{\rho C_p} \left( \frac{\partial^2 \theta}{\partial r^2} + \frac{1}{r} \frac{\partial \theta}{\partial r} \right) \quad (9)$$

where dimensionless temperature  $\theta = \frac{T-T_w}{T_{in}-T_w}$ , and subjected to following boundary condition for uniform wall temperature for pipe flow, case considered are

At the wall,  $r = R, \theta = 0$  for  $z > 0$

At the Centre,  $r = 0, \frac{\partial \theta}{\partial r} = 0$  for  $z \geq 0$

At the inlet,  $z = 0, \theta = 1$  for  $r \leq R$

where  $T$  temperature at any location within the pipe is the function of radial position  $r$  and axial location  $z$ ,  $\rho$  is density,  $C_p$  is heat capacity,  $\lambda$  thermal conductivity (Tanner, 1985).

All the fluid properties assumed the constant within the given equation, there are not any closed kind solutions to the present downside that take account of the temperature dependent viscosity.

Lyche and Bird (1956) solved and presented the complete solution in graphical form, for Newtonian fluid as well as for shear thinning fluid with consistency index of  $n = 0.5, 0.66$  and  $0$  (see, for example, Chhabra & Richardson, 1999).

## 2.3 CFD Modelling

Consider the case of thermal laminar flow through the pipe; all the property of fluid is constant except the temperature dependent viscosity. The governing equations (Bird, Armstrong, Hassager, & Curtiss, 1987) are the equation of continuity

$$\nabla \cdot U = 0 \quad (10)$$

where  $U$  is the velocity vector and the equation of motion

$$\rho \frac{DU}{Dt} = -\nabla p + \nabla \cdot \eta \dot{\gamma} + \rho g \quad (11)$$

where  $t$  time,  $g$  gravitational acceleration, can be neglected here for horizontal flow and the energy equation

$$\rho C_p \frac{DT}{Dt} = \nabla \cdot (\lambda \nabla T) + \frac{1}{2} \eta (\dot{\gamma} : \dot{\gamma}) \quad (12)$$

For low velocities as considered in this study, viscous dissipation term extremist right hand facet can be neglected, so it is not considered for the calculation. Eqs. (10), (11) and (12) can be combined with an appropriate viscosity function (Eqs. (7) and (8)) fully describe the problem.

For a flow in a tube subjected to transverse sinusoidal vibration in the  $x$ -direction of the form

$$x = A \sin(2\pi f t) \quad (13)$$

The boundary condition at the wall (wall velocity) in  $x$ -direction can be derived from equation (13) and can be written as:

$$\dot{x} = A 2\pi f \cos(2\pi f t) \quad (14)$$

The flow considered here is laminar, incompressible and fully developed. Reynolds number for internal pipe can be expressed as:

$$Re = \frac{\rho \bar{w} D}{\mu_{eff}} \quad (15)$$

where  $\mu_{eff} = k \left( \frac{3n+1}{4n} \right)^n \left( \frac{8\bar{w}}{D} \right)^{n-1}$  (Chhabra & Richardson, 1999) is the apparent viscosity of power-law type fluid and at  $n = 1$ , this viscosity equation can be used for Newtonian fluid. It helps to find the same relationship between the flow rate and pressure drop as given in Eqs. (5) and (6). Vibrational Reynolds number may be the most critical parameters for vibrational flow, this gives the assurance that flow remained laminar in the transverse direction also, at the given values of vibrational parameters and is given by

$$Re_v = \frac{\rho A 2\pi f D}{\eta} \quad (16)$$

## 3. CFD SIMULATION

Commercial software package ANSYS 16.2 was used for CFD simulations. CFD simulation basically divided into three following steps: 1) Pre-processor-ICEM CFD 16.2 was used to create flow geometry and meshing. 2) CFX solver used for analysis; Analysis was done for both Newtonian and power-law fluid by considering temperature dependent viscosity which was described by Eqs. (7) & (8), and 3) post-processing was performed within the CFD post processor tool out there in ANSYS.

### 3.1 Geometry and Grid Generation

Straight pipe of 20 mm diameter considered for the analysis. Food processing application like thermal sterilisation are generally performed in the pipe of diameter, considered here (Jung & Fryer, 1999; Liao, Rao, & Dutta, 2000). Three surface boundaries: Wall, inlet and outlet assign to a 500 mm length of the pipe. This length is sufficient to capture the effect of heat transfer effects (Easa & Barigou, 2010; Easa & Barigou, 2011).

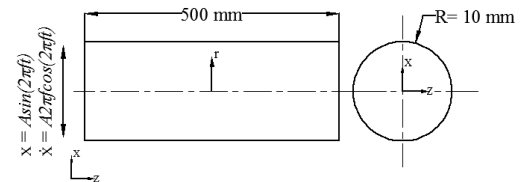


**Fig. 1. Geometry used for analysis showing the direction of vibration imposed on wall of the pipe.**

Structured grid with hexahedral cells was generated using ICEM-CFD 16.2. Grid independence studies were performed to fix the appropriate grid size in radial and axial direction as well, generally this study was taking place by considering coarse grid size to refining it until results were no longer reliant on its size. Approximately 4000 hexahedral cells per centimeter tube length and near about 1100 cells

across the tube section were confirmed after grid independence study. The fluid region nearer to the wall are considered most critical regions and therefore, at this region smallest size of grid used for better capturing the effect of the different variables where high gradient of velocity and temperature exist; 0.05 mm thickness and 1.1 factor of the increment were applied as indicated in Figure (2).

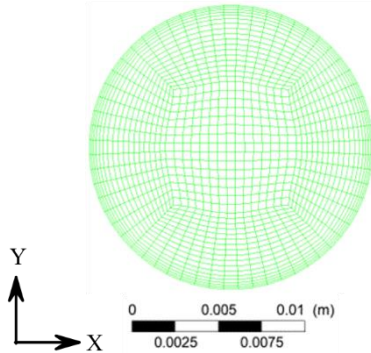


Fig. 2. Section of the Meshed geometry of pipe.

### 3.2 Flow Specification and Simulation Setting

Flow specification was performed using CFX-Pre. To reduce to computational time, assurance of fully developed velocity profile so that heat transfer effects can be captured in a shorter pipe, and vibration effects can be clearly demonstrated (Easa & Barigou, 2010; Easa & Barigou, 2011). The problem was solved in three steps: 1. Steady state flow simulation performed, where inlet velocity was calculated from Eq. (15) and  $T_{in} = 20^{\circ}C$  and ; 2. Velocity and temperature profile obtained from step (1) used as inlet boundary conditions for the second simulation; 3. Transient mode simulation setting was used for vibrational flow and run it for residence time of fluid into the pipe. For oscillating wall boundary condition, mesh deformation option in CFX was used which ensure the relative motion between the cells of the grid. Equation (13) and its first derivative i.e. Eq. (14) was used to define mesh displacement and boundary velocity, respectively and second step solution was used as an initial solution of the transient mode simulation.

Table 1 Range of the parameters used for simulation of flow.

Fluid	Newtonian	Power-law
D (mm)	20	20
$f$ (Hz)	50	50
A (mm)	2	2
L (mm)	500	500
$k_o$ (Pa s <sup>n</sup> )	$5e^{-7}$	$5e^{-5}$
$E_a$ (kJ mol <sup>-1</sup> )	35	35.00
$n$ (-)	1.0	0.8
$Re$ (-)	150-400	150-400
$\rho$ (kg m <sup>-3</sup> )	1000	1000
$C_p$ (J kg <sup>-1</sup> K <sup>-1</sup> )	4180	4180
$\lambda$ (W m <sup>-1</sup> K <sup>-1</sup> )	0.668	0.668

Zero gauge pressure condition applied at the outlet

of the pipe. No-slip and a constant wall temperature  $T_w = 140^{\circ}C$  were assigned at the wall. Simulations were carried out for different Reynolds numbers (Table 1), to capture the effect of radial mixing of temperature with varying Reynolds number.

To meet the requirements of boundedness and accuracy, High-resolution advection scheme and 'Backward Euler schemes of the second-order' transient scheme were selected respectively (Barth & Jespersen, 1989). The simulation time depends on the residence time of flow which was varying from low Reynolds number to high Reynolds number used for simulation. Total residence time was divided into equal time steps, 0.02 second required for the frequency of 50 Hz to complete one cycle and this cycle time was divided by 12 to obtain the equal time step which is  $1.6667 \times 10^{-3} s$ , used for the calculations. Simulation was executed for different value of time steps and found that by increasing the time steps, simulation time increases more with negligible increment in the solution accuracy. Convergence criteria were set for all residuals to  $10^{-4}$  root mean square (RMS) at each time steps which is a good level of accuracy.

## 4. VALIDATIONS OF CFD MODEL

To assure the high level of accuracy of the CFD model, although CFX codes are well validated, The Computational model reported here is validated for different conditions in the following sections. Validation of Computational model is done by making comparison either with theoretical data or with experimental data from literature where possible.

### 4.1 Adiabatic Isothermal Steady and Vibrational Flow

Equations (5) & (6) was used for making the comparison of CFD results obtained for laminar isothermal steady flow and the results are shown in Table 2. The percentage error calculated as  $\left(\frac{\Delta p_{CFD} - \Delta p_{Theory}}{\Delta p_{Theory}}\right) \times 100$ , indicating excellent agreement with correct consistent procedures classified roughly  $\pm 1\%$  (Easa & Barigou, 2008).

$$k = k_o \exp\left(\frac{E_a}{R_g T}\right)^n \text{ (Pa s}^n\text{)}, \text{ where } k_o = 5e^{-7}$$

$(Pa s^n)$  for  $n = 1.0$  &  $5e^{-5}(Pa s^n)$  for  $n = 0.8$   
Theoretical velocity profile of one-dimensional fully developed steady flow, which is given by Eqs. (3) & (4) was used to compare the CFD results obtained here. Both profiles match with the good level of accuracy.

Experimental results of the non-Newtonian (power-law type) isothermal fluid flow through pipe was used to validate the CFD model of vibrational flow (Figure 4). Deshpande and Barigou (2001) have applied longitudinal vibration on the pipe for different type of non-Newtonian fluid flow and presented the results in terms of flow enhancement ratio,  $E_R$  which is the ratio of time-averaged flow rate of vibrational flow to flow rate of steady flow.

**Table 2 Comparison between theoretical and CFD predictions of pressure difference for a range of Reynolds Number**

Velocity ( $m s^{-1}$ )	$n$ (·)	$k^*$ ( $Pa s^n$ )	$\Delta p_{Theory}$ ( $Pa$ )	$\Delta p_{CFD}$ ( $Pa$ )	% Error
0.0998	1.0	0.8616	3439.5	3455.3	0.46
0.1497	1.0	0.8616	5159.2	5189.1	0.58
0.1995	1.0	0.8616	6875.5	6922.9	0.68
0.2661	1.0	0.8616	9170.8	9234.9	0.69
0.1114	0.8	0.2286	500.43	504.31	0.78
0.1562	0.8	0.2286	655.81	661.12	0.81
0.1985	0.8	0.2286	794.40	801.15	0.81
0.2523	0.8	0.2286	962.43	971.57	0.95

\*Calculated at  $T = 20^\circ C$  from Eq. (8)

At higher frequency, results obtained by CFD shows slightly deterioration from the experimental results because, experimental condition used, the vibration was quite severe and lateral vibrations were unavoidable, hence Enhancement ratio predicted by CFD results was somewhat greater than experimental results. Later Easa and Barigou (2008) validated his work using CFX 10.0.

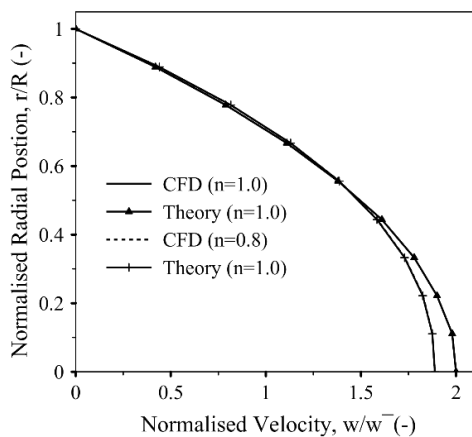


**Fig. 3. Validation of radial velocity profile of Newtonian fluid ( $n=1$ ) and Power-law fluid ( $n=0.8$ ).**

Deshpande and Barigou (2001) experimentally confirmed that flow rate enhancement of Newtonian fluid was unaffected by mechanical vibrations and CFD results also agree with this argument.

Through CFD, Tian (2015) has made comparison among three mode of vibration (rotational, longitudinal and transverse vibration), which is imposed on pipe wall. Figure (5) shows the good level of accuracy achieved with same setting opted by Tian (2015) for transverse vibrational flow. The work validated through CFD because no experimental data available in this regard (Easa & Barigou, 2008; Easa, 2009; Tian, 2015).

Following three cases are considered here to validate the flow through pipe with heat transfer:

(i) Temperature profile in the axial direction at different radial locations was analytically validated for isoviscous laminar Newtonian fluid flow, as shown in Figure (6), by using the equation (4) & (9).

Reference problem for validation was taken from Jakob (1949).

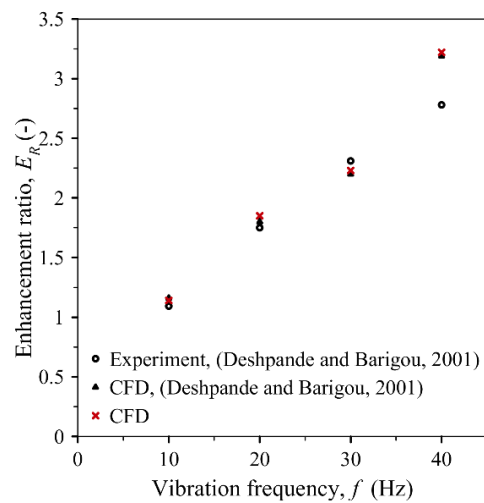


**Fig. 4. CFD validation with experimental results: flow rate enhancement of longitudinal vibrational flow of power-law fluid:  $k = 1.47 Pa s^n$ ;  $n = 0.57$ ;  $\rho = 1000 kg m^{-3}$ ;  $A = 1.60 mm$ ;  $\Delta p/L = 9.81 kPa m^{-1}$ .**

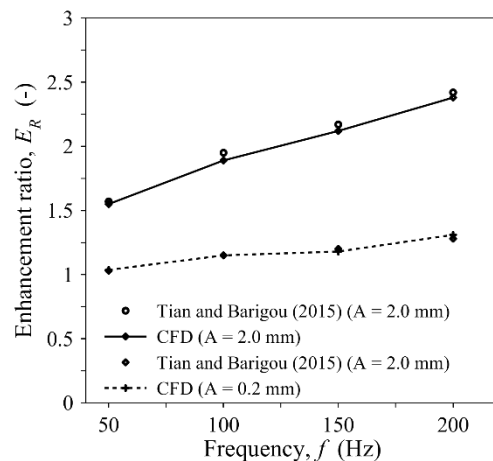


**Fig. 5. Validation of CFD results with Tian and Barigou (2015) results: flow rate enhancement of transverse vibrational flow of power-law fluid:  $k = 1 Pa s^n$ ;  $n = 0.6$ ;  $\rho = 1000 kg m^{-3}$ ;  $A = 2.0 mm$  &  $0.2 mm$ ;  $\Delta p/L = 20 kPa m^{-1}$ ;  $D = 4 mm$ ;  $L = 100 mm$ .**

## 4.2 Non-Isothermal Steady Flow Through Pipe

(ii) Temperature profile in the radial direction at given axial locations was analytically validated for isoviscous laminar Newtonian and power-law fluid flow, as shown in Figure (7), by using the equation (9). Reference problem used for validation was taken from Lyche and Bird (1956). They were the first, who validated and tabulated the solution of Equation (9).

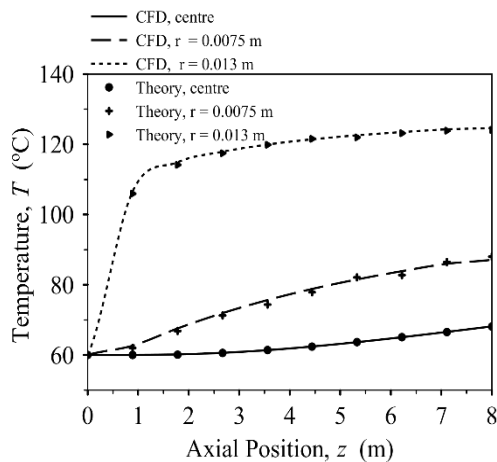


**Fig. 6. Validation of CFD results with theoretical expression (Equation 9); temperature profile in axial direction at different radial locations:  $T_{in} = 60\text{ }^{\circ}\text{C}$ ;  $T_w = 140\text{ }^{\circ}\text{C}$ ;  $D = 30\text{ mm}$ ;  $\bar{w} = 0.04\text{ m s}^{-1}$ ;  $\mu = 0.001\text{ Pa s}$ ;  $\rho = 998\text{ kg m}^{-3}$ ;  $C_p = 4180\text{ J kg}^{-1}\text{K}^{-1}$ ;  $\lambda = 0.668\text{ W m}^{-1}\text{K}^{-1}$ .**

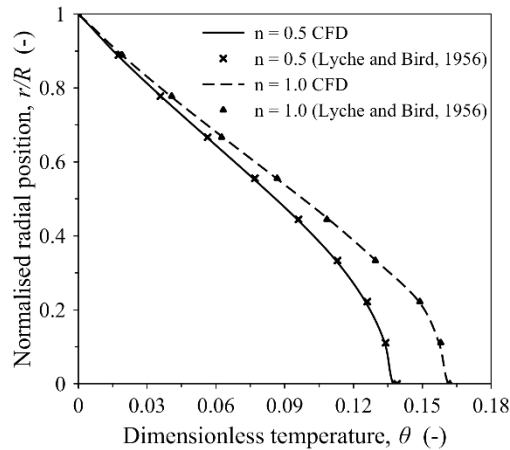


**Fig. 7. Validation of CFD results with theoretical expression (Equation 9); temperature profile in radial direction: ( $n = 1$ ;  $\mu = 1.0\text{ Pa s}$ ); ( $n = 0.5$ ;  $k = 1.0\text{ Pa s}^n$ );  $T_{in} = 27\text{ }^{\circ}\text{C}$ ;  $T_w = 127\text{ }^{\circ}\text{C}$ ;  $Gr = 5.24$   $\bar{w} = 0.01\text{ m s}^{-1}$ ;  $\rho = 1000\text{ kg m}^{-3}$ ;  $C_p = 4180\text{ J kg}^{-1}\text{K}^{-1}$ ;  $\lambda = 0.668\text{ W m}^{-1}\text{K}^{-1}$ .**

(iii) Validation of non isoviscous temperature profile, as considered was also necessary because temperature dependent viscosity has the great impact

on the flow field of fluid. Experimental results obtained from Kwant *et al.* (1973) was used to validate CFD results, as shown in Figure (8). Velocity profile becomes flattened compared to that obtained under isothermal condition.

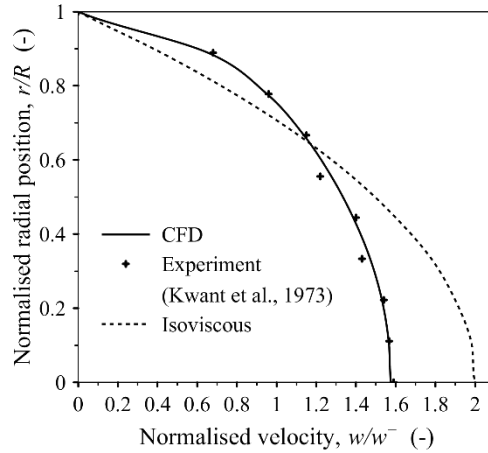


**Fig. 8. Experimental validation of velocity profile obtained from CFD results for non isoviscous; Newtonian fluid; steady state flow subjected to heat transfer:  $T_{in} = 27\text{ }^{\circ}\text{C}$ ;  $T_w = 127\text{ }^{\circ}\text{C}$ ;  $L = 1900\text{ mm}$ ;  $\mu = 1.3 \exp [1.49(T - 25\text{ }^{\circ}\text{C}) / (T_w - T_{in})]\text{ Pa s}$ ;  $\bar{w} = 0.09\text{ m s}^{-1}$ ;  $n = 1$ ;  $\rho = 1000\text{ kg m}^{-3}$ ;  $C_p = 4180\text{ J kg}^{-1}\text{K}^{-1}$ ;  $\lambda = 0.668\text{ W m}^{-1}\text{K}^{-1}$ .**

## 4.3 Non-Isothermal Unsteady Vibrational Flow Through Pipe

CFD predicted results for isothermal steady state Newtonian and non-Newtonian fluid was, first, experimentally validated by Deshpande and Barigou (2001) and found worthy level of accuracy, at intervals roughly  $\pm 10\%$ , for a variety of rheological behaviors and under a wide range of vibration conditions, later Easa and Barigou (2008), Tian and Barigou (2015) has also done the work in this regard.

Excellent level of accuracy can be achieved through CFD when codes tested for non-isoviscous steady state laminar flow as discussed in previous section. There are, however no experimental and analytical data available on vibrational flow subjected to heat transfer. Validation of various CFD models for different flow conditions in previous sections supports the argument that CFD codes are reliable and robust for the purpose of studying heat transfer effects on the flow considered here under the vibration.

## 5. RESULT AND DISCUSSION

Simulation results for the laminar flow with heat transfer of a Newtonian fluid and power law fluid with non-isoviscous flow through tube with an isothermal wall, subjected to transverse vibration with a frequency of  $50\text{ Hz}$  and the amplitude of vibration  $A = 2\text{ mm}$  are discussed in the flowing sections:

### 5.1 Effect of Reynolds Number on Heat Transfer of Newtonian Fluid.

Usual feature of viscous flow was confirmed from simulation of the steady flow of a Newtonian fluid with non-isoviscous viscosity shown in Figure (9a) that shows high temperature gradient near wall, while in the core region of pipe, temperature remains virtually at its inlet value, which results non uniform heating or cooling of fluid. This is undesirable condition for the processes like thermal sterilisation, etc.

Vorticity in the  $xy$  plane can be increased through transverse vibration which increases the radial mixing of fluid, results increase the radial temperature distribution shown in Figure (9b) (Easa & Barigou, 2011).

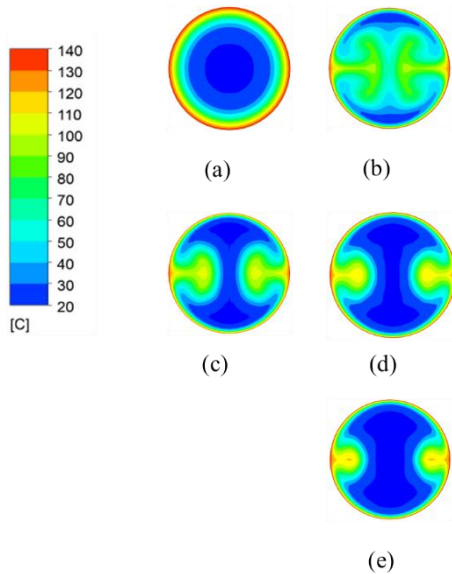


**Fig. 9. Radial temperature distribution contours for Newtonian fluid (a) Steady flow (b) Vibrated flow at  $Re = 150$  (c) Vibrated flow at  $Re = 225$  (d) Vibrated flow at  $Re = 300$  (e) Vibrated flow at  $Re = 400$   $f = 50$  Hz;  $A = 2$  mm;  $D = 20$  mm;  $L = 500$  mm;  $\mu = 5 \times 10^{-7} \exp\left(\frac{E_a}{R_g T}\right)$  (Pa s);  $n = 1.0$ ;  $T_{in} = 20^\circ\text{C}$ ;  $T_w = 140^\circ\text{C}$ .**

Vibration creates swirling or spiraling motion in the fluid which enhances heat transfer by promoting convection. Swirling effect was dominated by increasing flow velocity (Reynolds number) in axial direction, as shown in Figure (9) and (10), which decreases the radial mixing in the perpendicular to the direction of vibration, leads to non-uniform temperature distribution and increases the thermal entrance length. Figure 11 also supports the above statement, as initially, Ratio of area-averaged temperature of vibrated flow ( $T_{VF}$ ) to steady flow ( $T_{SF}$ ) decreases exponentially for all the cases, while that of increases rapidly. Ratio of that temperature at the tube exit decreases from  $\sim 1.14$  to  $\sim 1.03$  as the Reynolds number increases to 400 from 150. In other words, these temperature ratio effects depend on the axial velocity of fluid, at lower velocity ( $Re 150$ ) temperature of the fluid start increasing at about

$\sim 20\%$  length of the pipe, whereas this length increased about  $\sim 80\%$  as Reynolds number increases to 400. To achieve desire temperature distribution, either vibrational amplitude, Vibration frequency or length of the pipe can be increased (Easa & Barigou, 2011).

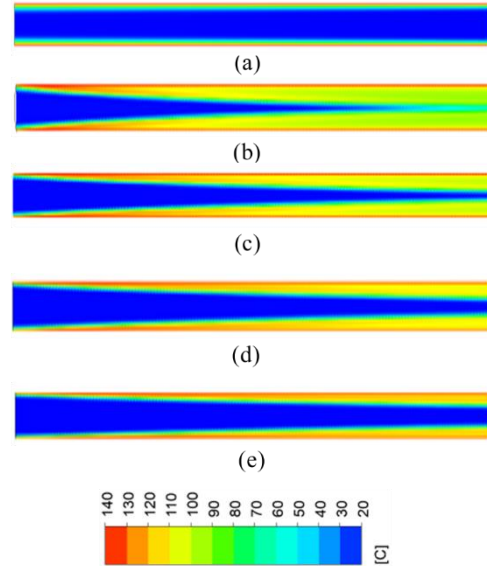


**Fig. 10. Contours of temperature distribution along the pipe for Newtonian fluid (a) Steady flow (b) Vibrated flow at  $Re = 150$  (c) Vibrated flow at  $Re = 225$  (d) Vibrated flow at  $Re = 300$  (e) Vibrated flow at  $Re = 400$ .  $f = 50$  Hz;  $A = 2$  mm;  $D = 20$  mm;  $L = 500$  mm;  $\mu = 5 \times 10^{-7} \exp\left(\frac{E_a}{R_g T}\right)$  (Pa s);  $n = 1.0$ ;  $T_{in} = 20^\circ\text{C}$ ;  $T_w = 140^\circ\text{C}$ .**

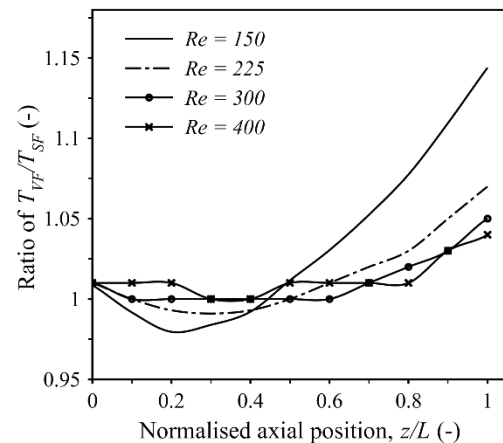


**Fig. 11. Ratio of area-averaged temperature of vibrated flow ( $T_{VF}$ ) to steady flow ( $T_{SF}$ ) with varying Reynolds number along the pipe:  $f = 50$  Hz;  $A = 2$  mm;  $D = 20$  mm;  $D\mu = 5 \times 10^{-7} \exp\left(\frac{E_a}{R_g T}\right)$  (Pa s);  $n = 1.0$ ;  $T_{in} = 20^\circ\text{C}$ ;  $T_w = 140^\circ\text{C}$ ;  $L = 500$  mm.**

### 5.2 Effect of Reynolds Number on Heat Transfer of Power Law Fluid.

Pre-exponential factor ( $k_o = 5 \times 10^{-5}$ ) considered

here was such that the apparent viscosity of non-Newtonian fluid is approximately equal to the viscosity of Newtonian fluid (Eqs. (7) and (8)) so that comparisons has been made among the fluid considered.

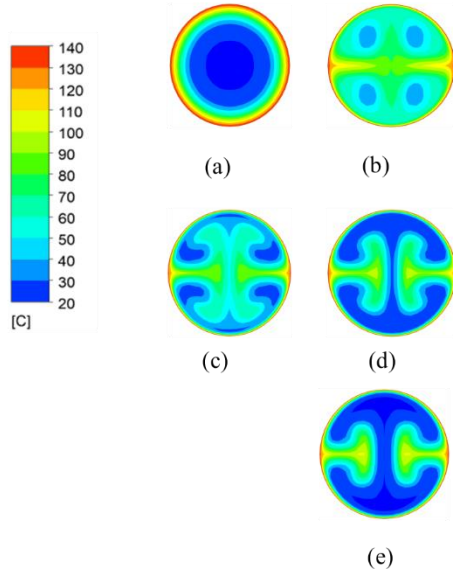


**Fig. 12. Radial temperature distribution contours for Power law fluid (a) Steady flow (b) Vibrated flow at  $Re = 150$  (c) Vibrated flow at  $Re = 225$  (d) Vibrated flow at  $Re = 300$  (e) Vibrated flow at  $Re = 400$ .  $f = 50$  Hz;  $A = 2$  mm;  $D = 20$  mm;  $\mu = 5 \times 10^{-5} \exp\left(\frac{E_a}{R_c T}\right)^n$  (Pa s $^n$ );  $n = 0.8$ ;  $T_{in} = 20^\circ\text{C}$ ;  $T_w = 140^\circ\text{C}$ ;  $L = 500$  mm.**

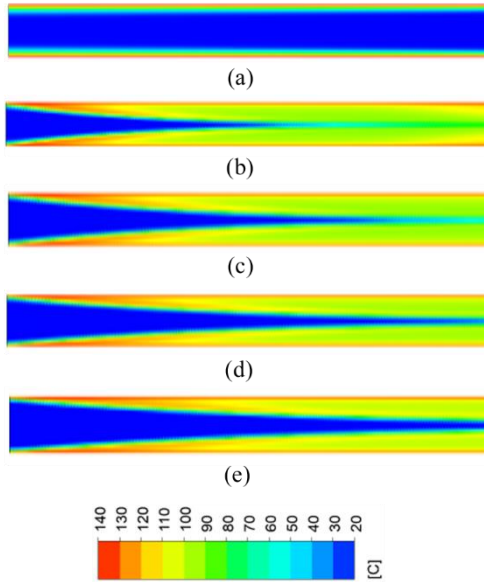


**Fig. 13. Temperature distribution contours along the pipe for Power law fluid (a) Steady flow (b) Vibrated flow at  $Re = 150$  (c) Vibrated flow at  $Re = 225$  (d) Vibrated flow at  $Re = 300$  (e) Vibrated flow at  $Re = 400$ .  $f = 50$  Hz;  $A = 2$  mm;  $D = 20$  mm;  $k = 5 \times 10^{-5} \exp\left(\frac{E_a}{R_c T}\right)^n$  (Pa s $^n$ );  $n = 0.8$ ;  $T_{in} = 20^\circ\text{C}$ ;  $T_w = 140^\circ\text{C}$ ;  $L = 500$  mm.**

Temperature contours for  $n = 0.8$ , across the section were shown in Figure (12), demonstrate the shear thinning flow behavior at different Reynolds number. As  $n$  (from  $n = 1.0$  to  $n = 0.8$ ) reduces, the viscosity of the fluid at a given shear rate is lower by virtue of the increased shear thinning. The power law fluid has more uniform temperature distribution across the pipe; such effects decrease as the condition of zero pseudo plasticity, i.e.  $n = 1.0$  shown in Figure (9). But comparisons among the cases of power law fluid considered; radial mixing decreases with increasing to flow velocity same as for Newtonian fluid (Figure 13).

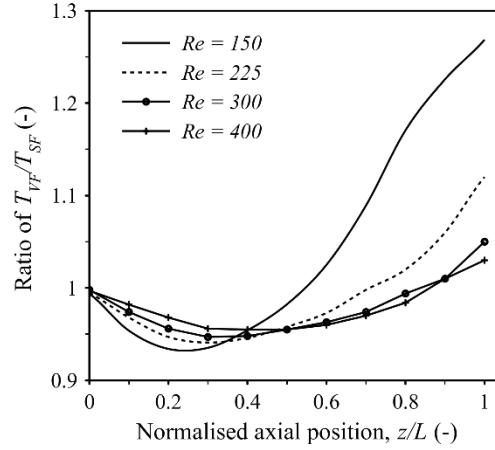


**Fig. 14. Ratio of area-averaged temperature of vibrated flow ( $T_{VF}$ ) to steady flow ( $T_{SF}$ ) with varying Reynolds number along the pipe:  $f = 50$  Hz;  $A = 2$  mm;  $D = 20$  mm;  $k = 5 \times 10^{-5} \exp\left(\frac{E_a}{R_c T}\right)^n$  (Pa s $^n$ );  $n = 0.8$ ;  $T_{in} = 20^\circ\text{C}$ ;  $T_w = 140^\circ\text{C}$ ;  $L = 500$  mm.**

Unlike the Newtonian fluid; Temperature distribution along the pipe (Figure 14) was increasing more rapidly, this results shows that as increasing the shear thinning behavior, requirement of the long pipe gets reduces and more uniform temperature distribution can be achieved.

Based on the temperature values obtained from the CFD results, following equations are used to calculate the wall heat transfer coefficient, those are present in Table (3).

$$\dot{m}C_p(T_{out} - T_{in}) = ha\Delta T_m \quad (17)$$

$$\Delta T_m = \frac{(T_w - T_{out}) - (T_w - T_{in})}{\ln[(T_w - T_{out}) / (T_w - T_{in})]} \quad (18)$$

where  $\dot{m}(= \rho\pi R^2\bar{w})$  is the mass flow rate,  $T_{out}$  is the area-averaged temperature at the pipe exit and  $a (= 2\pi RL)$  is the wall surface area of the pipe.

Through transverse vibration, which produces the chaotic fluid motion and swirling effects, adequate radial mixing across the tube can be achieved which leads to great addition in heat transfer, which is the function of vibration parameter (frequency and amplitude) and Reynolds number used, getting numerous folds comparatively for low Reynolds number. Ratio of Heat transfer coefficient of vibrational flow,  $[\text{h}]_v$  to steady state flow, as a

function of Reynolds number are plotted in Figure 15. In spite of the small number of data points, these trends clearly validate the observations made so far that the vibrational effects reduce in significance as Re increases for both the fluid considered.

**Table 3 Compression of heat transfer coefficient under vibrated flow:  $A = 2 \text{ mm}$ ;  $L = 500 \text{ mm}$ ;  $D = 20 \text{ mm}$ ;  $k = k_o \exp\left(\frac{E_a}{R_c T}\right)^n (\text{Pa s}^n)$ ;  $k_o = 5e^{-7} (\text{Pa s}^n)$  for  $n = 1.0$ ;  $k_o = 5e^{-5} (\text{Pa s}^n)$  for  $n = 0.8$**

$Re^*$ (-)	$n$ (-)	$h$ ( $W m^{-2} K^{-1}$ )	$h_v$ ( $W m^{-2} K^{-1}$ )	$h_v/h$ (-)
150	1.0	425.52	817.42	1.92
225	1.0	490.63	724.38	1.48
300	1.0	540.84	750.83	1.39
400	1.0	595.09	797.42	1.34
150	0.8	419.19	1316.32	3.14
225	0.8	469.86	938.98	1.99
300	0.8	535.44	768.43	1.44
400	0.8	548.66	757.15	1.38

\*Calculated at  $T = 140^\circ\text{C}$

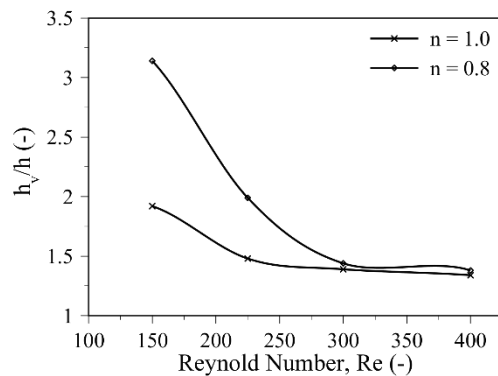


**Fig. 15. Variation of heat transfer coefficient of vibrated flow with Reynolds Number.  $f = 50 \text{ Hz}$ ;  $A = 2 \text{ mm}$ ;  $D = 20 \text{ mm}$ ;  $L = 500 \text{ mm}$ ;  $\mu = 5 \times 10^{-7} \exp\left(\frac{E_a}{R_c T}\right) (\text{Pa s})$   $k = 5 \times 10^{-5} \exp\left(\frac{E_a}{R_c T}\right)^n (\text{Pa s}^n)$ ;  $n = 0.8$ ;  $T_{in} = 20^\circ\text{C}$ ;  $T_w = 140^\circ\text{C}$ .**

### CONCLUSION

Transverse vibration generates complex spiraling fluid motion and strong vorticity field on the steady laminar flow of a fluid in a tube. This method increases: heat transfer, a much more uniform radial temperature profile, a prompt development of temperature profile along the pipe.

A valid CFD model is employed to show that a transverse vibration has great influence when used for comparatively low Reynolds number, where vorticity has dominated in nature; as Reynolds number increases, uniformity of radial temperature profile, temperature profile along the pipe and heat transfer reduces significantly. To maintain such conditions either increase the vibration frequency or

vibration amplitude; but practically, it is very difficult to maintain such flow.

With reducing the flow behavior index i.e. more shear thinning ( $n < 1$ ) fluid, required less frequency and amplitude of vibration and comparatively shorter pipe to maintain flow with uniform radial temperature and more rapid temperature profile along the tube.

Further, this work can be extended in the following area: solid-liquid two phase or multiphase flow and more complex rheology of fluid such as Shear-thickening fluid, Herschel Bulky fluid, etc. to generalize the vibrational flow subjected to heat transfer.

### REFERENCES

- Barth, T. J. and D. C. Jespersen (1989). The design and application of upwind schemes on unstructured meshes. *AIAA: Paper*. 89,0366
- Bird, D. V., R. C. Armstrong, O. Hassager and C. Curtiss, (1987). *Dynamics of polymeric liquid, Fluid Mechanics (2nd ed., Vol. 1)*. New York: Wiley.
- Chhabra, R. P. and J. F. Richardson (1999). *Non-Newtonian flow in the process industries: Fundamentals and engineering applications*. Butterworth Heinemann.
- Christiansen, E. B. and J. S. Craig (1962). Heat transfer to pseudoplastic fluids in laminar flow. *AIChE J.* 8(2), 154-160
- Deshpande, N. S. and M. Barigou (2001). Vibrational flow of non-newtonian fluids. *chemical Engineering Science* 56, 3845-3853
- Easa, M. (2009). *CFD studies of complex fluid flows in pipes*. Ph.D. thesis. University of Birmingham, Birmingham, UK.
- Easa, M. and M. Barigou (2008). CFD analysis of viscous non-Newtonian flow under the influence of a superimposed rotational vibration. *Computers & Fluids* 37(1), 24-34
- Easa, M. and M. Barigou (2010). Enhancing radial temperature uniformity and boundary layer development in viscous Newtonian and non-Newtonian flow by Transverse oscillations: A CFD study. *Chemical Engineering Science* 65(6), 2199-2212
- Easa, M. and M. Barigou (2011). CFD simulation of transverse vibration effects on radial temperature profile and thermal entrance length in laminar flow. *AIChE Journal* 57(1), 51-56
- Hobbs, D. M. and F. J. Muzzio (1997). The Kenics static mixer: a three-dimensional chaotic flow. *Chemical Engineering Science* 67(3), 153-166
- Jung, A. and P. J. Fryer (1999). Optimising the quality of safe food: Computational modelling of a continuous sterilisation process. *Chemical Engineering Journal* 54, 717-730
- Kreith, F. and M. S. Bohn (1986). *Principles of Heat*

- transfer* (4th ed.). New York: Harper & Row.
- Kwant, P. B., R. Fierens and A. Van Der Lee (1973b). Non-isothermal lamiar flow - II. Experimental. *Chemical Engineering Science* 28(6), 1317-1330
- Kwant, P. B., A. Zwaneveld and F. C. Dijkstra (1973a). Non-isothermal laminar pipe flow - I. Theoretical. *Chemical Engineering Science* 28(6), 1303-1316
- Liao, H. J., M. A. Rao and A. K. Dutta (2000). Role of thermo-rheological behaviour in simulation of continuous sterilisation of a starch dispersion. *Trans IChem E* 78(C), 48-56
- Lyche, B. C. and R. B. Bird (1956). The Graetz-Nusselt problem for a power-law non-Newtonian fluid. *Chemical Engineering Science* 6(1), 35-41
- Saatdjian, E., A. Rodrigo and J. Mota (2012). On chaotic advection in a static mixer. *Chemical Engineering Journal* 18(7), 289-298
- Shrirao, P. N., R. U. Sambhe and P. R. Bodade (2013). Convective heat transfer analysis in a circular tube with different types of internal threads of constant pitch. *International Journal of Engineering and Advanced Technology* 2(3), 335-340.
- Steffe, J. F. (1996). *Rheological methods in food process engineering* (2 ed.). Freeman Press.
- Tanner, R. I. (1985). *Engineering Rheology*. Oxford: Clarendon Press.
- Tian, S. (2015). *CFD modelling of oscillatory perturbed advection in viscous flows*. Ph.D. thesis. University of Birmingham, Birmingham, UK.
- Tian, S. and M. Barigou (2015). An improved vibration technique for enhancing temperature uniformity and heat transfer in viscous fluid flow. *Chemical Engineering Science* 123, 606-619.